OBSERVATION OF NOISE OF FAN WITH OBSTACLE FOR ELECTRIC COMPONENTS

Kimihisa KANEKO, Satoshi MATSUMOTO, Tsutomu YAMAMOTO

[1] *Fuji Electric Co., Ltd., Center of Innovative Technology, Corporate R&D Headquarters, 1, Fuji-machi Hino, Tokyo, 191-8502, Japan*

SUMMARY

This paper presents the use of experimental and numerical simulations to observe the noise made by a fan used to cool electrical components when interacting with an obstacle. A simplified experimental setup was designed consisting of three parts: a fan, a duct, and an obstacle. The one-block obstacle in the experimental model was assumed to be an aggregate electric component. The sound pressure level (SPL) was found to be influenced by the distance between the obstacle and the fan, and the compressible Large Eddy Simulation (LES) approach was used to predict the SPL. The numerical simulation captured the influence of the obstacle on the SPL of the fan. This method was found to be applicable for predicting the SPL when developing low-noise products.

INTRODUCTION

The recent trend in downsizing electric equipment has caused an increase in the heat generation density and an accompanying need to increase air flow to enable cooling. Therefore, the aerodynamic noise from the fan is the dominant source of noise in air-cooled electrical equipment. Fan noise is known to be influenced by the fan operating point and the fan's surrounding structures [1-3]. It is important to predict the noise level when designing electronic equipment incorporating a fan, and to understand aerodynamic noise phenomena under various practical conditions. However, it is difficult to derive such knowledge from the sound source without considering the structure of the electric components and the fan. The authors' previous study focused on the noise from a fan with a non-axisymmetric structure to understand the noise generation mechanism relating to the electronic equipment [4].

To conduct a numerical analysis of aerodynamics noise, either the hybrid computational aeroacoustics (CAA) method or the direct CAA method can be employed. The hybrid CAA method can be assumed to separately solve incompressible turbulent flow and the acoustic wave. In

addition, turbulent fluctuation, which is the source of acoustic propagation, can be obtained using several turbulent models: the Large Eddy Simulation (LES), Detached Eddy Simulation (DES), and the Unsteady Reynolds Averaged Navier-Stokes (U-RANS), and acoustic propagation can be obtained using Lighthill's acoustic analogy. The effectiveness of using the hybrid CAA method in analyzing aerodynamic noise from a centrifugal fan [5-7] and an axial flow fan [8, 9] has been previously reported.

However, the direct CAA method uses compressible Navier–Stokes equations to compute both the turbulent flow and the acoustic wave, but it requires high-accuracy numerical schemes to resolve turbulent and acoustic fluctuations. Investigations using the cavity flow under a high Mach number 0.7 and Reynolds number 41000 have been conducted [10] using a direct numerical simulation and high-accuracy schemes. In our study, the direct CAA method is used to consider the aeroacoustic interactions between the fan and the obstacle under a low Mach number flow.

EXPERIMENTAL METHOD

Experimental Setup

Various component layouts can be considered when designing the internal structure of air-cooled electronic devices, and the choice depends on the device being designed. However, it is always necessary to maintain a short distance between the device and the fan to enable effective heat dissipation from electric components, and electronic components need to be placed in a limited area with respect to circuit design requirements. A typical electronic device structure is illustrated in the conceptual diagram in Figure 1. Electronic components block the air flow and alter ventilation resistance. In this basic study of the influence of obstacles on noise, the obstacles are assumed to have a block shape and to block air flow. When a device structure is designed, the distance between the fan, the electronic component block, and the height of the block are often designated. Here, dependence of the fan and its noise performance on distance, *x*, between the fan and the block and the height, *h*, of the block are studied, and experimental parameters are shown in Table 1.

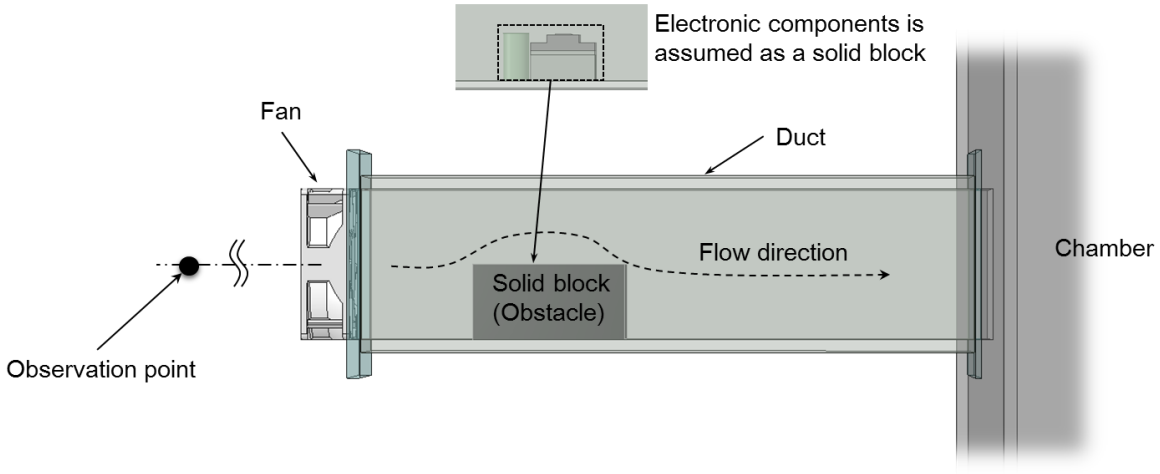

Figure 1: Experimental Setup

Fan performance was measured using a method complying with ISO 5801, Industrial Fans-Performance Testing Using Standardized Airways [11]. The experiment was set-up in a hemi-anechoic room. The performance of the fan when an obstacle was present in the flow channel was obtained by initially measuring ventilation resistance caused by the obstacle and then applying correction to the measurement. Noise emitted by the assisting blower in the chamber, shown in

Figure 1, was negligible compared to fan noise, as acoustic materials were used on the internal chamber wall. The sound pressure level (SPL) was measured using a microphone placed both 1 m in front of the fan and placed on the rotating fan axis. The observed SPL spectra frequency range were 5 kHz. The Hanning-window time domain was applied prior to Fast Fourier Transform (FFT). Finally, the SPL of each condition was observed using an A-weighted adjusting frequency.

Table 1: Experimental parameter

Parameter definition	Value
Blade number	5
Strut number	7
Blade diameter *D* [mm]	113
Rotational Speed [m/s]	35
Duct height *H* [mm]	120
Duct width *W* [mm]	120
Duct length *L* [mm]	500
Obstacle height *h/H* [-]	0.5
Obstacle length *l/H* [-]	1.0
Obstacle distance from the fan *x/D* [-]	0.1, 0.2, 0.3, 0.4 0.5, 0.75, 0.9, 1.0, 1.5, 2.0
Mach number	0.1
Reynolds number	1×10^5

NUMERICAL METHOD

Direct CAA

The LES of the compressible Navier–Stokes equation was employed with the direct CAA, which requires a large amount of computational resources to compute. Mass, momentum, and energy conservation were also used. As density fluctuation under compressible flow is influenced by temperature and pressure, ideal gas dynamics were employed in these equations. Temperature fluctuation was assumed to be negligible at a low Mach number in our conditions, and under this assumption, mass and momentum conservation were employed. Density was defined using the ideal gas law, and temperature was defined using previous Unsteady Reynolds Averaged Navier-Stokes (U-RANS) computation results. The HELYX ver.2.2 [13], which is part of Open FOAM software [14], was used to compute these equations.

To evaluate acoustic propagation to the free space at the observation point, the above mesh resolution was used, as shown in Figure 2. The computational domain is divided into several regions, depending on the dominant physical phenomena used to control mesh density. This mesh has a quadrangular pyramid shape, the bottom and apex of which lie on the inlet of the fan and near the observation point, respectively. Resolution of the mesh used in numerical calculation changes, depending on whether the mesh is used to calculate turbulent flow or aerodynamic noise. Dominant turbulent fluctuation occurs near the fan and downstream from it, and a mesh resolution of Δx = 0.2 mm is used near the rotating blade. To observe dominant acoustic propagation between the fan and the SPL observation point, a mesh resolution of Δx = 2 mm is used with a total number of 15 million cells. A turbulence model LES of unsteady flow is also employed, and one equation eddy model [15] is used for the sub-grid scale LES model. The second-order upwind difference scheme for is chosen for the advection term and the second-order backward scheme is chosen for temporal

discretization. To obtain an enhanced frequency resolution, the time-step is set to 1×10^{-5} sec, and the mesh resolutions of the acoustic fields, time step, and numerical schemes are determined in advance using simple 2-dimensional domain computation.

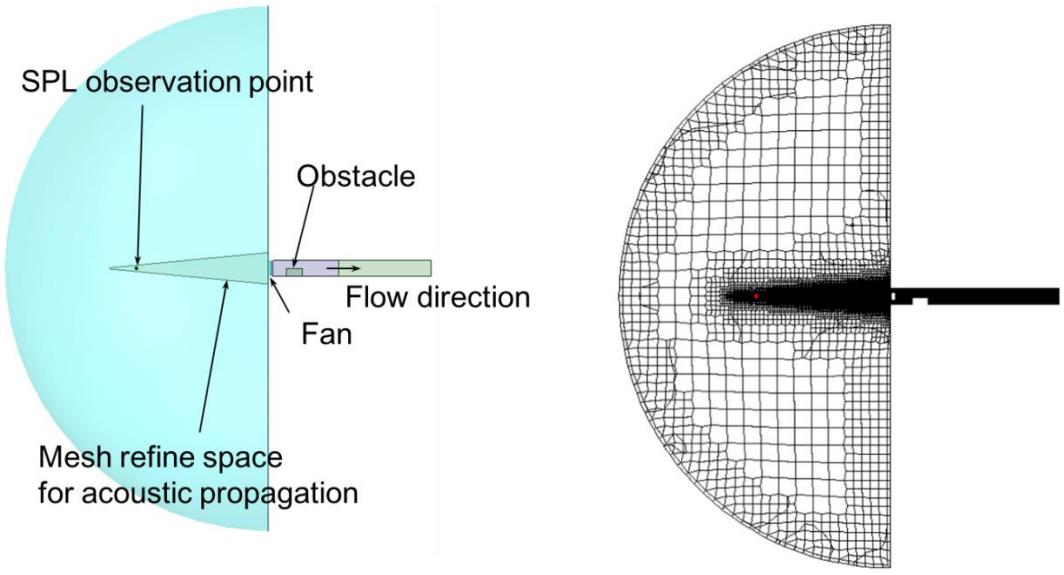

(a) Computational domain *(b) Mesh*

Figure 2: Computational domain and mesh

RESULTS AND DISCUSSION

Experimental results

Figure 3 shows measurement results of fan performance. Max and min of *x/D* are indicated, and to illustrate the effect of the obstacle, the result without an obstacle is also shown. To clarify the change in fan performance with respect to the presence of the obstacle, system resistance with the obstacle was measured in advance and the result was used for data correction.

Performance of the fan with an obstacle placed at a large distance from the fan, $x/D = 2.0$, was almost equivalent to that without an obstacle: there was no influence from the obstacle. However, the fan's performance deteriorated when the obstacle was placed near the fan, $x/D = 0.1$, particularly with a high flow coefficient. It appears that the performance of the fan deteriorated when the outlet flow from the fan collided with the obstacle and returned to the fan, thereby disturbing flow around the blades.

Figure 4 shows the overall SPL using the same conditions presented in Figure 3. SPL was increased at a low flow rate ($\varphi < 0.2$) due to separation flow occurring on the blades. Furthermore, SPL was increased with decreasing *x/D*.

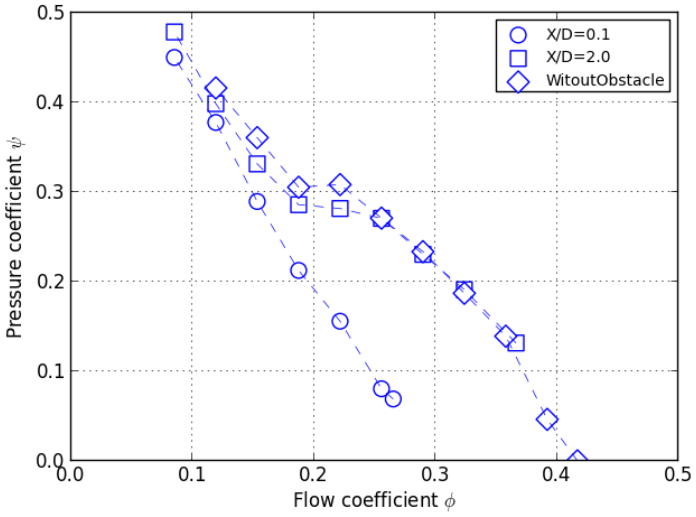

Figure 3: Fan performance

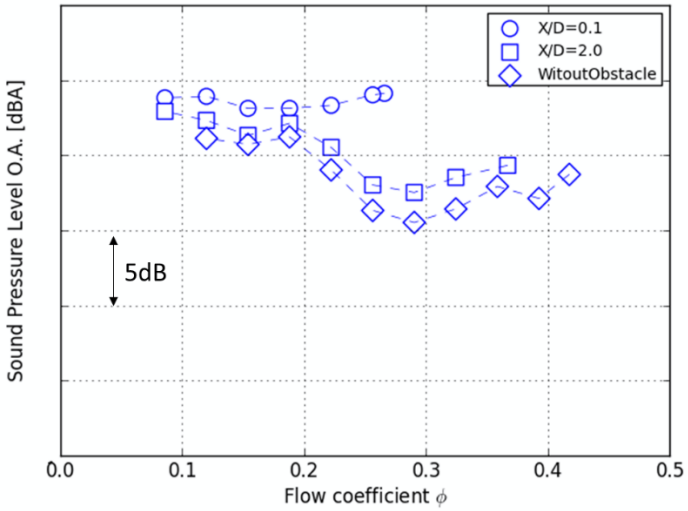

Figure 4: Overall SPL

Numerical simulation results

Figure 5 shows the instantaneous pressure fluctuations at the central cross section of the analysis area. The pressure wave propagated radially on the upstream side space of the fan, and the pressure distribution near the fan corresponded with blade rotation. Therefore, pressure decreased when the suction side of the blades passed the reference cross section and increased when the inter-blade space passed the reference cross section.

The computed overall SPL at each distance is shown in Figure 6. The horizontal axis indicates the distance from the fan axis to the fan inlet face, and the vertical axis indicates the overall SPL, which is the calculated pressure fluctuation at each location. Each SPL was obtained along the sound attenuation curve. Figure 7 shows the computed and measured SPL spectral density at the observation point. The computed SPL was calculated from the pressure fluctuation. The rotation speed, N_0, of the fan was 95 Hz, and the blade passing frequency (BPF) was 475 Hz. The dominant frequency, $4N_0$, and BPF could be observed without use of the duct or the obstacle [4], and depending on the length of the duct, several dominant frequencies were observed.

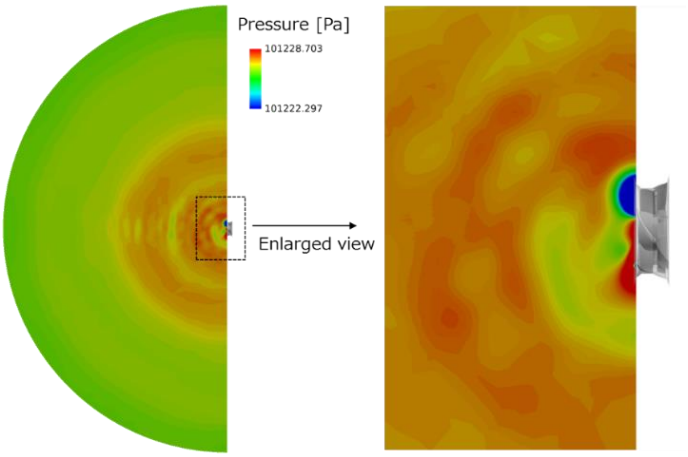

Figure 5: Instantaneous pressure distribution and SPL (x/D = 0.3, φ = 0.22)

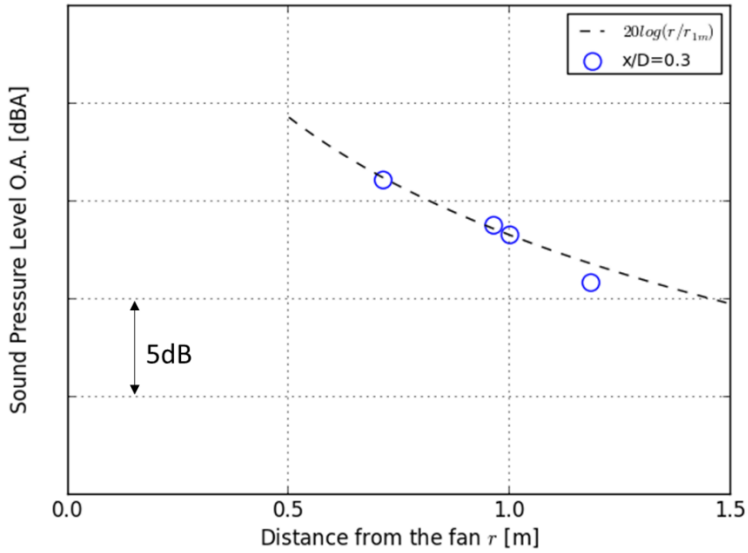

Figure 6: SPL and distance from fan (x/D = 0.3,φ = 0.22)

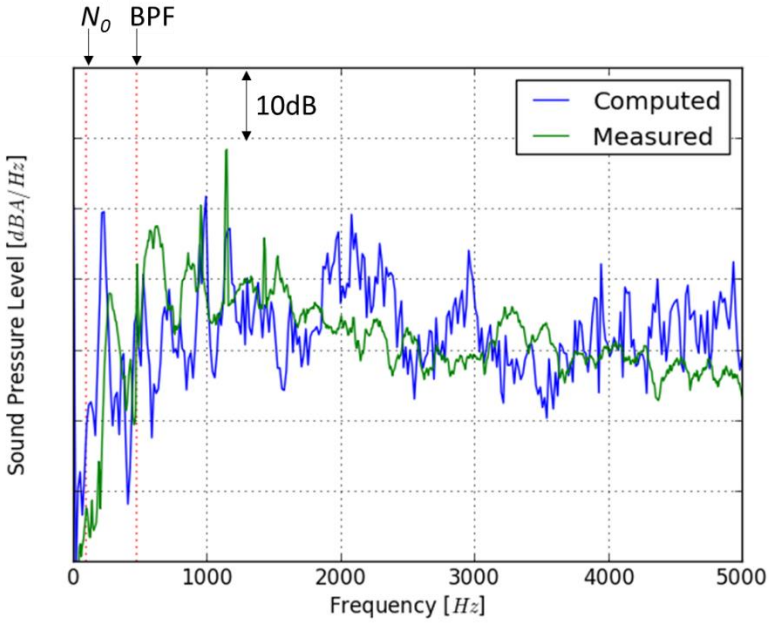

Figure 7: SPL spectra at observation point (x/D = 0.3, φ =0.22, r = 1.0 m)

The overall SPL values for various *x/D* at φ = 0.22, 0.26, and 0.29 are shown in Figure 8, together with computed results of typical conditions of φ = 0.22. SPL increased with a decreasing flow coefficient and drastically increased when *x/D* was 0.5 or less. This trend was also reflected in the computational results.

Therefore, the numerical analysis shows that N_0 can affect the pressure increase caused when the flow from the outlet of the fan collides with the obstacle. The low sound pressure level at N_0, which was determined by measurements, could be related to the influence of the small space between the obstacle and the wall and the air-passing sound relating to the obstacle. However, there was an increase in SPL at *x/D* = 1.5 compared to *x/D* = 0.9 and 2.0, because SPL increased at a dominant frequency, particularly at approx. 1130 Hz.

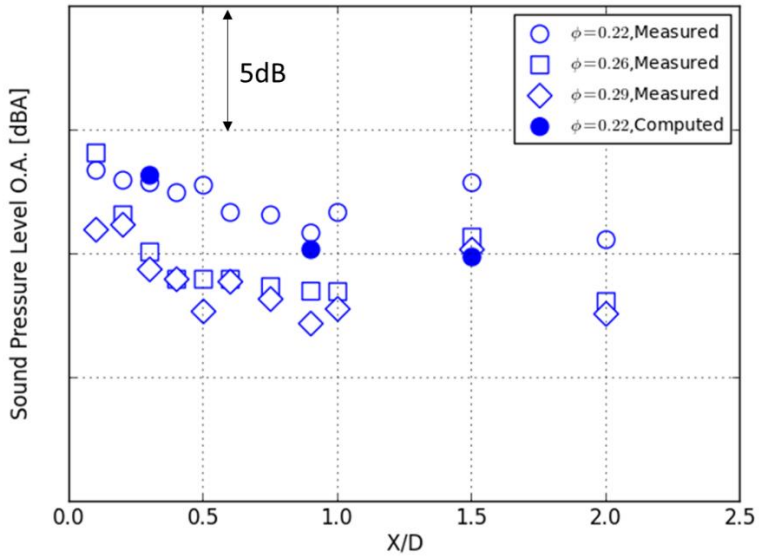

Figure 8: SPL at each x/D

Figure 9 shows an instantaneous vorticity isosurface colored using velocity magnitudes and representing different obstacle distances under the same flow coefficient conditions. Vorticity distributed near the blade tip was more pronounced at *x/D* = 0.3 compared to with other conditions. When *x/D* = 0.3, a large vorticity was formed in the area on the downstream side of the fan in a vertical direction at the lower part of the duct, and in a horizontal direction at the upper part, which caused a large imbalance in the flow at the outlet area of the fan. This could cause a change in the discharge angle at the outlet of the blades and degradation of the fan performance.

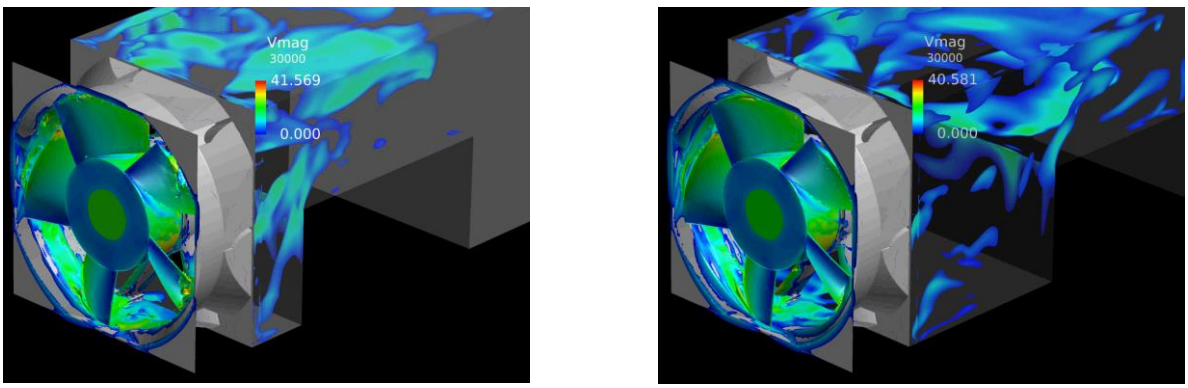

(a) x/D = 0.3 *(b) x/D = 0.9*

Figure 9: Instantaneous vorticity distribution (φ= 0.22)

ACKNOWLEDGMENTS

This research was supported using the computational resources of the K computer and other computers of the High-Performance Computing Infrastructure (HPCI) system provided by the RIKEN Advanced Institute for Computational Science (AICS) and (the names of the HPCI System Providers) within the HPCI System Research Project (Project ID: hp150143).

BIBLIOGRAPHY

[1] H. Reese, T. Carolub – *Axial fan noise: towards sound prediction based on numerical unsteady flow data - a case study.* Acoustics 08 Paris, pp 4069-4074, **2008**

[2] K. Kawaguchi, K. Okui, M. Kuwaumi –*Effects of Turbulence of Inlet Flow on Performance of Compact Axial Flow Fan (Effect of Turbulence Generated by Obstacle on Fan Characteristic and Noise).* Turbomachinery, vol. 35, No. 8, pp.32-40, **2007**

[3] Fukue T., Koizumi K, Ishizuka M. and Nakagawa S., – *The effects of Electronic Enclosure Inlet on P-Q Curves of In-stalled Axial Cooling Fans.* J. JSME, Vol. 75, No.755, pp.873-880, **2009**

[4] K. Kaneko, T. Yamamoto, C. Kato –*Aerodynamic noise simulation of axial flow fan with non-axisymmetric structure for power electronics equipment.*, The 13th Asian International Conference on Fluid Machinery 7th - 10th September **2015**

[5] S. Caro, R. Sandboge, J. Iyer, Y. Nishino, –*Presentation of a CAA formulation based on Lighthill's analogy for fan noise.* Fan Noise 2007 Conference, pp.17-19, **2007**

[6] Y. Guo, C. Kato, Y. Yamade, Y. Ohta, T. Iwase, R.Takayama – *Computation of Noise from Internal Flow in a Centrif-ugal Fan*. Seisan Kenkyu, Vol. 66, No. 1, pp27-31, **2014**

[7] T. Iwase, H. Obara, H. Yoneyama, T. Kishitani, Y. Yamade, C. Kato –*Prediction of aerodynamic noise for centrifugal fan of air-conditioner.* FAN 2015, Lyon (France), 15-17 April, **2015**

[8] T. Takayama, C. Kato – *Numerical Prediction of Aerodynamic Noise Radiated from Propeller Fan.* Institute of Industrial Science The University of Tokyo, vol. 63, No. 1, pp. 61-64, **2011**

[9] S. Bianchi, D. Borello, A. Corsini, F. Rispoli, A. Sheard –*Large-Eddy Simulation of the Aerodynamic and Aeroacoustic Perfomance of a Ventilation Fan.* Advances in Acoustics and Vibration, vol. 2013, Article ID 876973, **2013**

[10] X. Gloerfelt, C. Bailly, D. Juve, – *Direct computation of the noise radiated by a subsonic cavity flow and application of integral methods*, Journal of Sound and Vibration, Vol 266, Issue 1, 4, Pages 119-146, Sept. **2003**

[11] Japanese Industrial Standards Committee, – *Testing methods for turbo-fans*, JIS B8330, **2000**

[12] C. Kato, – *Direct Numerical Simulation of Turbulent Flows.* Turbomachinery, vol. 42, No.5, pp.290-296, **2014**

[13] https://engys.com/

[14] http://www.openfoam.com

[15] Won-Wook Kim and Suresh Menon, – *A new dynamic one-equation subgrid-scale model for large eddy simulations.* AIAA 95-0356, **1995**